

RESEARCH ARTICLE

The Effects of ASMase Mediated Endothelial Cell Apoptosis in Multiple Hypofractionated Irradiations in CT26 Tumor Bearing Mice

Hong Zhu^{1&}, Kai Deng^{2&}, Ya-Qin Zhao¹, Xin Wang¹, Ya-Li Shen¹, Tai-Guo Liu¹, Dan-Dan Cui¹, Feng Xu^{1*}

Abstract

Background: To investigate the effects of ASMase mediated endothelial cell apoptosis in multiple hypofractionated irradiations in CT26 tumor bearing mice. **Materials and Methods:** Thirty-five CT26 tumor bearing mice were subjected to single ionizing radiation (IR) of 0, 3, 6, 9, 12, 15, 18 Gy. Eight hours after IR, the mice were sacrificed and tumor tissues were used for CD31 immunohistochemistry staining, TUNEL and CD31 double staining, ASMase activity assay. Then 6 and 12 Gy were chosen for multiple hypofractionated IR experiments according to the above results. Each time after IR, 5 mice were sacrificed and assayed as above. **Results:** The ASMase activities were increased significantly after a single IR of 12 Gy or higher which was accompanied with remarkable increased endothelial cell apoptosis and decreased MVD. For 6 Gy which was not high enough to trigger ASMase activation, after 2 or more times of IR, the ASMase activities were significantly increased accompanied with remarkable increased endothelial cell apoptosis and decreased MVD. While for 12 Gy, after 2 or more times of IR, the ASMase activities and endothelial cell apoptosis rates were maintained without remarkable increase; however, the MVD was significantly decreased. What's more, the cancer cell apoptosis rates were significantly increased after multiple IR for both 6 Gy and 12 Gy. **Conclusions:** ASMase mediated endothelial cell apoptosis may play an important role in the process of multiple hypofractionated IR for CT26 colorectal carcinoma.

Keywords: ASMase - endothelial cell - hypofractionated irradiations - CT26 tumor bearing mice

Asian Pac J Cancer Prev, 16 (11), 4543-4548

Introduction

For decades, DNA has been considered as the main cellular target of deleterious effects of ionizing radiation (IR) (Pollard and Gatti, 2009). Nevertheless, molecular signals initiated at cellular membranes are now identified as critical events in a large spectrum of radiation-induced cellular processes (Corre et al., 2010). If IR provokes DNA damage directly by energy deposit on the DNA double helix and indirectly by reactive species, origin of IR induced molecular events initiated at the plasma membrane remains more obscure.

Recently, studies have highlighted that acid sphingomyelinase (ASMase), which generates ceramide from sphingomyelin, is involved in modulation of membrane structures and signal transduction after IR (Garcia-Barros et al., 2003; Corre et al., 2010; Zeidan and Hannun, 2010). They found that ceramide generation from the ASMase activation was independent of the DNA damage following IR (Gulbins and Kolesnick, 2003). One of the most reliable cell models is the endothelial cell apoptosis after exposure to high dose IR (Garcia-

Barros et al., 2003; Garcia-Barros et al., 2010). ASMase has been found in almost all cell types that have been studied (Truman et al., 2011), however, the endothelium is a particularly rich source which synthesizes 20 times as much as any other cells in the body (Pena et al., 2000; Garcia-Barros et al., 2003; Truman et al., 2010). Many investigations demonstrated that radiation doses higher than 8-10 Gy induces rapid apoptosis of tumor vascular endothelial cells by activating ASMase (Park et al., 2012; Lan et al., 2013), leading to secondary death in tumor cells. Besides, this effect was further confirmed in microvascular endothelium in lung, brain and small intestines (Pena et al., 2000; Li et al., 2003; Rotolo et al., 2008; Corre et al., 2010; Hua and Kolesnick, 2013). Nevertheless, all the studies were carried out in single dose IR. In fact, hypofractionated radiotherapy which was delivered in multiple times was very popular in the clinical treatment of cancers such as prostate cancer (Chapet et al., 2013), rectal cancer (Koukourakis et al., 2011), lung cancer (Osti et al., 2013), and so on. So it's very important to investigate the effects of ASMase mediated endothelial cell apoptosis in multiple hypofractionated IR.

¹Department of Medical Oncology, ²Department of Gastroenterology, West China Hospital, Sichuan University, Chengdu, Sichuan Province, China [&]Equal contributors *For correspondence: fengxuster@gmail.com

Materials and Methods

Cell culture

CT26 cell line was kindly provided by the State Key Laboratory of Biotherapy, Sichuan University (Sichuan Province, China) and was cultured in RPMI-1640 supplemented with 10% (v/v) fetal bovine serum plus 100 µg/ml amikacin. The cells were maintained in the 37°C humidified incubator with 5% CO₂ atmosphere.

Design of animal experiments

Female BALB/c mice (6-8 weeks age) weighing between 16 and 18 g were purchased from Experimental Animal Center of Sichuan University (Sichuan Province, China). All animal procedures were approved by the Animal Care and Scientific Committee of Sichuan University. In 0.1 ml of PBS, about 105 CT26 cells were suspended and inoculated into the rear flank of mice to establish tumor models. After 14 days, when the tumors were about 0.5 cm in diameter, 35 mice were randomized into the 7 groups (five mice per group) to receive different doses of single IR: 0, 3, 6, 9, 12, 15, 18 Gy. Eight hours after the IR, all the mice were sacrificed and the tumors were excised immediately to frozen in liquid nitrogen. The tumors were then subjected to CD31 immunohistochemistry staining, terminal deoxynucleotidyl transferase dUTP nick end labeling (TUNEL) and CD31 double staining, and ASMase activity assay. According to the above results, 6 and 12 Gy were chosen for further studies. Fourteen days after incubation, 25 tumor bearing mice were randomized into 5 groups (five mice per group) to 1 time, 2 times, 3 times, 4 times, and 5 times of IR (6 Gy per time). Another 15 tumor bearing mice were randomized into 3 groups (five mice per group) to receive 1 time, 2 times and 3 times of IR (12 Gy per time). Eight hours after the finish of the respective IR, the mice were sacrificed and the tumors were also disposed as above.

Irradiation

The IR treatments were conducted with the ELEKTA Synergy linear accelerator (Zeng et al., 2012). The 6-MeV x rays with source-to-surface distance of 100 cm were applied with 2 cm bonus for all the experiments. Before IR, each mouse was anesthetized by 5% chloral hydrate and was shielded by a lead cover with only the tumor exposed.

Determination of microvascular density

The tumor tissues obtained from CT26 tumor-bearing mice were fixed, paraffin embedded, and cut into 3- to 5-mm sections. The sections were used for CD31 staining and TUNEL and CD31 double staining. Immunohistochemical staining of CD31 was performed according to the manufacturer's instructions. The anti-CD31, a mouse monoclonal antibody (dilution 1:200; ZSGB-BIO CO., LTD, Beijing, China) was used for microvessel staining.

Microvessel density (MVD) was employed for angiogenesis assessment (Li et al., 2012). Immunostained tumor sections were scanned at low power magnification (40× and 100×) to identify the areas which represented the highest vascular density - so called "hot spots" (Zhu et al.,

2011). MVD was measured in three to five fields with a higher density of CD31-positive cells and cell clusters at 200× magnification. The presence of a visible blood vessel lumen was not required to be defined as positive (Saponaro et al., 2013). The average vessel count in three to five examined hot spots per section was considered the value of MVD. All counts were performed by three investigators in a blinded manner. Microvessel counts were compared between the observers and discrepant results were reassessed. The consensus was used as the final score for analysis.

Determination of endothelial and cancer apoptosis cells

Apoptotic cells in the tumor tissues were identified via TUNEL assay using an in situ apoptotic cell detection kit (Roche, USA) following the manufacturer's instructions (Bruns et al., 2002). Briefly, sections were covered with diluted proteinase K, incubated for 20 min at 37°C, and washed with phosphate-buffered saline (PBS) two times, each for 5 min. Next, they were incubated with TUNEL reaction mixture (terminal deoxynucleotidyl transferase (TdT) buffer: TdT end-labeling cocktail = 1: 9) for 60 min at 37°C and washed with PBS. Then, sections were added with converter POD and incubated at 37°C for 30 min. After washed with PBS for three times, substrates were added for colorization. Next, sections were blocked with 5% bovine serum albumin (BSA). At last, they were subjected to CD31 immunohistochemistry as described above. Sections were viewed under microscopy (LEICA DM1000, Germany), and pictures were taken at 200× magnification. Nuclei of cancer apoptotic cells were stained into brown, while endothelial apoptotic cells showed brown nuclei with a red cytoplasm tail. Apoptotic cells were counted at least 5 randomly selected fields. The apoptotic index was defined as follows: apoptotic index (%) = 100% × cancer or endothelial apoptotic cells / total cells.

Determination of ASMase activity

The activity levels of ASMase were assayed using trinitrophenylaminolauroyl (TNPAL)-sphingomyelin (Sigma-Aldrich) referring previous literature (Xu et al., 2010). For assaying ASMase, acid buffer (pH 5.0) was prepared (100 mM sodium acetate, 0.1% Triton X-100, and 0.01 M ethylenediaminetetraacetic acid). The samples were homogenized in cold acid buffer. The resulting homogenates were centrifuged, and the supernatants were used for determination of ASMase activity and protein concentration. For each assay, 30 ml of the supernatant was added to a tube containing 10 mg of TNPAL-sphingomyelin in 200 ml of the above acid buffers. The reaction was stopped by adding 750 ml mixture of isopropanol-heptane-5% H₂SO₄ (40:10:1, vol/vol/vol). Next, 400 ml of heptane was added and the tube was shaken and then centrifuged to separate the two phases. The upper phase contained TNPAL-ceramide, which was formed from TNPAL-sphingomyelin by the ASMase present in the sample. The absorbance of the heptane phase was read at 330 nm using a Spectra-Max Plus (BIO-RAD, USA). ASMase activity was expressed in nanomoles of ceramide per hour per milligram of protein.

Protein content was measured with a bicinchoninic acid protein assay kit (Sigma-Aldrich) according to the manufacturer's instructions.

Statistical analysis

Results were expressed as the mean±standard deviation (SD). Statistical comparisons of mean values were analyzed by one-way ANOVA, followed by the Student's t-test. All statistical analyses were performed using the SPSS 16.0 software package. All *P*-values were two-sided and *P*<0.05 was considered as the significant level of difference.

Results

The MVD, endothelial and cancer cells apoptosis rates, and ASMase activity after single IR

The MVD of tumor tissues after 0, 3, 6, 9, 12, 15, and 18 Gy of single IR were 103.60±8.35, 98.20±13.37, 94.6±14.05, 88.40±12.05, 70.06±10.01, 61.20±10.62, and 50.60±12.66, respectively (Figure 1A, C). It's slightly lower in 12, 15, and 18 Gy groups than other groups (*P*<0.05). The endothelial apoptosis rates were 0.08±0.03%, 0.26±0.09%, 0.25±0.08%, 0.38±0.09%, 1.18±0.11%, 1.45±0.18%, and 1.87±0.22% respectively in 0, 3, 6, 9, 12, 15, and 18 Gy groups (Figure 1B, D). From the

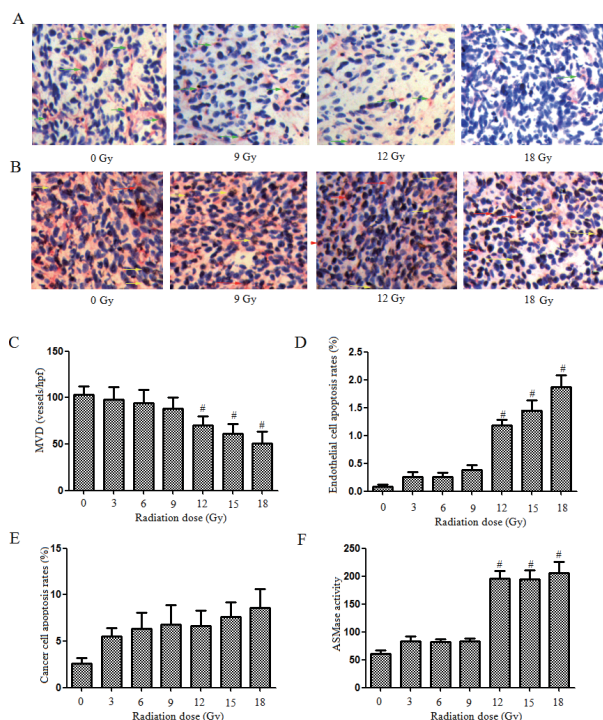


Figure 1. Various doses of single IR. A. CD31 immunohistochemistry staining. Representative pictures after IR of 0, 6, 12, and 18 Gy were presented. Cytoplasm of endothelial cells were stained into red (green arrow). B. TUNEL and CD31 double staining. Representative pictures after IR of 0, 6, 12, and 18 Gy were presented. Nuclei of cancer apoptotic cells were stained into brown (yellow arrow), while endothelial apoptotic cells showed brown nuclei with a red cytoplasm tail (red arrow). C. histogram of MVD. D. histogram of endothelial apoptotic cells. E. histogram of cancer apoptotic cells. F. histogram of ASMase activity. #*P*<0.05 compared with those which received single IR of 0, 3, 6, 9 Gy

results, we can see that the endothelial apoptosis rates were significantly higher in 12, 15, and 18 Gy groups than other groups (*P*< 0.05). While the cancer cell apoptosis rates were 2.63%±0.56%, 5.50±0.92%, 6.33±1.74%, 6.77±2.10%, 6.64±1.67%, 7.61±1.59%, and 8.58±2.05% respectively in 0, 3, 6, 9, 12, 15, and 18 Gy groups (Figure 1B, E), and there was no significant difference for these groups except slightly lower in 0 Gy group. The ASMase activities were 61.20±5.50, 83.40±9.26, 81.80±5.36, 83.20±4.97, 196.20±12.91, 194.80±15.82, and 205.40±20.19 respectively in 0, 3, 6, 9, 12, 15, and 18 Gy groups (Figure 1F), and it's significantly higher in 12, 15, and 18 Gy groups than other groups (*P*<0.05).

The MVD, endothelial and cancer cells apoptosis rates, and ASMase activity after multiple IR of 6 Gy

The MVD of tumor tissues after 1, 2, 3, 4, and 5 times IR of 6 Gy were 94.20±10.35, 65.20±16.90, 40.20±8.81, 23.00±5.15, and 22.80±5.54, respectively (Figure 2A, C), and were decreased significantly with the IR times increase. The endothelial apoptosis rates were 0.31±0.09%, 1.19±0.26%, 1.77±0.23%, 1.48±0.35%, and 1.50±0.40% respectively in 1, 2, 3, 4, and 5 times IR

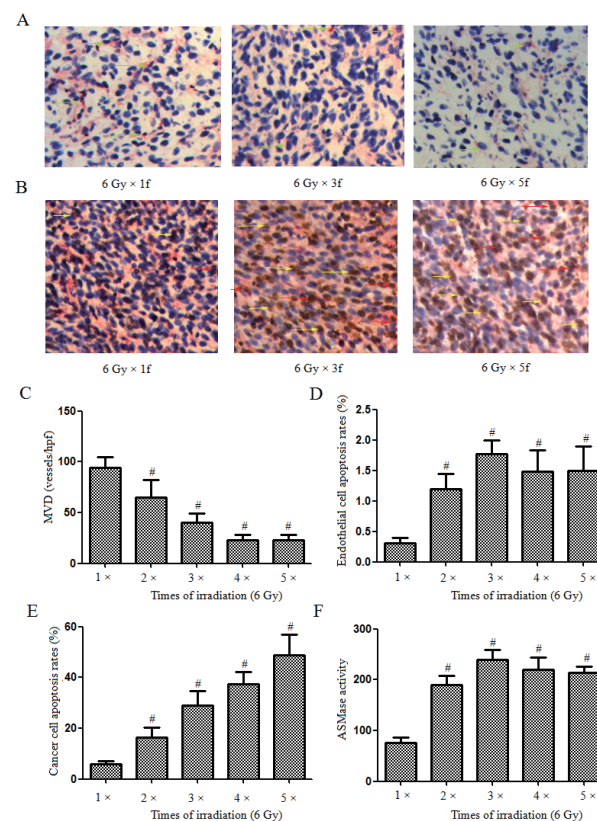


Figure 2. Multiple IR with dosage of 6 Gy. A. CD31 immunohistochemistry staining. Representative pictures after 1, 3, and 5 times IR of 6 Gy were presented. Cytoplasm of endothelial cells were stained into red (green arrow). B. TUNEL and CD31 double staining. Representative pictures after 1, 3, and 5 times irradiations of 6 Gy were presented. Nuclei of cancer apoptotic cells were stained into brown (yellow arrow), while endothelial apoptotic cells showed brown nuclei with a red cytoplasm tail (red arrow). C. histogram of MVD. D. histogram of endothelial apoptotic cells. E. histogram of cancer apoptotic cells. F. histogram of ASMase activity. #*P*<0.05 compared with those which received single time IR of 6 Gy

groups (Figure 2B, D). From the results, we can see that the endothelial apoptosis rates were significantly higher in multiple IR groups than single IR group ($P<0.05$). While the cancer cell apoptosis rates were $5.95\pm 1.19\%$, $16.42\pm 3.74\%$, $29.08\pm 5.71\%$, $37.38\pm 4.91\%$, and $48.72\pm 8.27\%$ respectively in 1, 2, 3, 4, and 5 times IR groups (Figure 2B, E), and were increased significantly with the IR times increase ($P<0.05$). The ASMase activities were 76.60 ± 10.50 , 190.20 ± 17.94 , 239.60 ± 19.97 , 219.60 ± 24.75 , and 214.20 ± 11.08 respectively in 1, 2, 3, 4, and 5 times IR groups (Figure 2F), and it's significantly higher in other groups than single time IR group ($P<0.05$).

The MVD, endothelial and cancer cells apoptosis rates, and ASMase activity after multiple IR of 12 Gy

The MVD of tumor tissues after 1, 2, and 3 times IR of 12 Gy were 72.60 ± 13.13 , 43.80 ± 6.98 , and 21.60 ± 6.58 , respectively (Figure 3A, C), and were decreased with the IR times increase. The endothelial apoptosis rates were $1.31\pm 0.39\%$, $1.68\pm 0.26\%$, and $1.41\pm 0.25\%$ respectively in 1, 2, and 3 times IR groups (Figure 3B, D). The endothelial apoptosis rate was slightly higher in 2 times IR group ($P<0.05$), however, no statistical difference was observed between other two groups ($P>0.05$). While the cancer cell apoptosis rates were $6.84\pm 1.22\%$, $21.83\pm 4.39\%$, and

$41.88\pm 5.48\%$ respectively in 1, 2, and 3 times IR groups (Figure 3B, E), and were increased significantly with the IR times increase ($P<0.05$). The ASMase activities were 198.00 ± 16.00 , 231.80 ± 24.39 , and 222.60 ± 34.57 respectively in 1, 2, and 3 times IR groups (Figure 3F), and no statistical difference was observed ($P>0.05$).

Discussion

Acid sphingomyelinase (ASMase, EC 3.1.4.12), primarily found in lysosomes, plays a central role in transmembrane signaling as well as in lysosomal metabolic functions (Truman et al., 2011). ASMase activation is required to promote enhanced cross-linking of surface receptors to initiate intracellular signaling events. ASMase activation is also implicated in lung development (Longo et al., 1997), in the signaling of stress responses to bacteria and viruses (Utermohlen et al., 2003), and in the apoptotic response of endothelial cells to IR (Garcia-Barros et al., 2003), to UV light (Zhang et al., 2001), and to chemotherapeutic drugs (Dimanche-Boitrel et al., 2005). In the context of an oxidative stress such as IR, the best example is the translocation of the enzyme ASMase from lysosomes to the outer layer of cell membrane, which then induces sphingomyelin hydrolysis and ceramide formation (Kolesnick and Fuks, 2003). As a second messenger, ceramide then mediated the following cell apoptosis (Stancevic and Kolesnick, 2010). Using membrane preparations of endothelial cells, it has been shown that IR raised a generation of ceramide by ASMase activation, an event totally decoupled from nuclear signaling (Haimovitz-Friedman et al., 1994). Use of genetic mouse model permit to definitely confirm that IR-triggered wave of apoptosis in microvascular endothelium in lung, brain and small intestines small was abolished by genetic ASMase invalidation (Santana et al., 1996; Pena et al., 2000; Paris et al., 2001). So ASMase played an important role in the process of endothelial apoptosis after IR.

However, ASMase activation is a dose dependent process. Richard Kolesnick and colleagues found that tumor response to single time IR was regulated by endothelial cell apoptosis in MCA/129 fibrosarcoma bearing mice, and this regulation happened only when the IR dose was higher than 8-10 Gy (Garcia-Barros et al., 2003). Nevertheless, they later found that the IR dose higher than 11-14 Gy could induce massive endothelial cells apoptosis in B16 melanoma bearing mice which significantly regulated the tumor response (Garcia-Barros et al., 2010). While Saral Spiegel and colleagues found that a single IR of 8 Gy could activate ASMase and therefore regulate the radiosensitivity of prostate cancer cell lines *in vitro* (Nava et al., 2000). In this study, we found that the ASMase activity was increased significantly after a single IR of 12 Gy which was accompanied with massive increased endothelial cell apoptosis and decreased MVD. However, these phenomena were not found in single IR of 9 Gy or lower dose group. So we think the single IR of dose higher than 9-11 Gy could activate ASMase activity and then regulate endothelial cell apoptosis in CT26 tumor bearing mice. Besides, the ASMase activation is

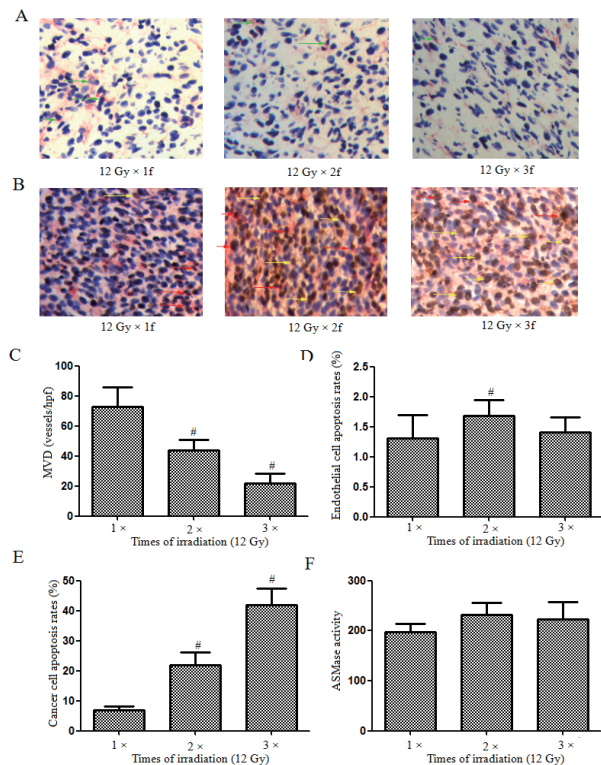


Figure 3. Multiple IR with dosage of 12 Gy. A. CD31 immunohistochemistry staining. Representative pictures after 1, 2, and 3 times IR of 12 Gy were presented. Cytoplasm of endothelial cells were stained into red (green arrow). B. TUNEL and CD31 double staining. Representative pictures after 1, 2, and 3 times IR of 12 Gy were presented. Nuclei of cancer apoptotic cells were stained into brown (yellow arrow), while endothelial apoptotic cells showed brown nuclei with a red cytoplasm tail (red arrow). C. histogram of MVD. D. histogram of endothelial apoptotic cells. E. histogram of cancer apoptotic cells. F. histogram of ASMase activity. # $P<0.05$ compared with those which received single time IR of 12 Gy

a time dependent process. In many cases, the increase in ASMase activity is transient, peaking within a few minutes and declining within an hour (Zeidan et al., 2008; Zeidan and Hannun, 2010). Many researchers found that diverse cells could activate ASMase and release ceramide within seconds to minutes after IR *in vitro* (Gulbins and Kolesnick, 2003; Rotolo et al., 2005; Truman et al., 2010). However, Samet et al. (1999) detected the ASMase activity in crude extracts of HL-60 cells, they found that the activity of ASMase at 37°C was linear with time for at least 5 h and it increased with time for at least 22h. Another *in vivo* study measured the ASMase activity of parotid gland after a single IR of 25 Gy, they found that the ASMase activity in parotid glands increased rapidly from 4 to 24h after IR, and then declined gradually after 1 to 2 weeks (Xu et al., 2010). Similar to this *in vivo* study, we found that the ASMase activities were still very high in 12, 15 and 18 Gy groups 8 hours after IR. The tumor cell apoptosis was slightly increased in IR groups than in control, however, no statistical significance was observed among these single IR groups.

According to the results of single IR study, we had chosen 6 Gy and 12 Gy for further multiple hypofractionated IR studies. For 6 Gy which is not high enough to trigger ASMase activation, after 2 or more times of IR, the ASMase activities were significantly increased accompanied with remarkable increased endothelial cell apoptosis and decreased MVD. While for 12 Gy, after 2 or more times of IR, the ASMase activities and endothelial cell apoptosis rates were maintained without remarkable increase; however, the MVD was significantly decreased. What's more, we found that the cancer cell apoptosis rates were significantly increased after multiple IR for both 6 Gy and 12 Gy. Past studies (Fuks and Kolesnick, 2005; Moeller et al., 2005) indicated that the endothelial cell damage induced by the low-dose (1.8-3 Gy) exposures of fractionated IR does not enhance tumor cell death effectively, as the death signaling pathway in endothelium is repressed by concomitant activation of tumor cell HIF-1. Reactive oxygen species generated by waves of hypoxia/reoxygenation occurring after each IR exposure lead to translation of HIF-1 mRNA transcripts stored in specialized cytosolic stress granules of hypoxic tumor cells. This adaptive response generates VEGF and other proangiogenic factors that attenuate IR induced apoptosis in endothelial cells. However, we found that 2 or more times of 6 or 12 Gy IR could effectively induce endothelial cell apoptosis and enhance tumor cell death. Nevertheless, it's maybe more difficult for lower dose to induce endothelial cell apoptosis, and this depends on different IR dosages, tumor types and so on.

The mechanism between hypofractionated IR with endothelial cell apoptosis and tumor cell death is still not for sure. One possible mechanism is that the endothelial cell apoptosis caused by hypofractionated IR lead to ischemia/hypoxia which then generate second damage to the tumor cells (Garcia-Barros et al., 2003). However, one recent study (Lan et al., 2013) found that ablative hypofractionated IR not only decreased MVD and hypoxia, but also normalized the tumor vasculature and then increased the vascular perfusion and the number of

pericyte-covered vessels. So the well oxygenated state of tumor cells may contribute to the enhanced tumor cell death. Nevertheless, the more detailed mechanism needs further studies.

In conclusion, the single IR with dose higher than 9-11 Gy could cause significant ASMase activation which was accompanied with remarkable increased endothelial cell apoptosis and decreased MVD in CT26 tumor bearing mice. Besides, 2 or more times of 6 or 12 Gy IR could also induce ASMase mediated endothelial cell apoptosis. ASMase mediated endothelial cell apoptosis may play an important role in the process of multiple hypofractionated IR for CT26 colorectal carcinoma.

Acknowledgements

This study was supported by grants from the National Natural Scientific Foundation of China (No. 81301962) and National Basic Research Program of China (2011CB935800).

References

- Bruns CJ, Shrader M, Harbison MT, et al (2002). Effect of the vascular endothelial growth factor receptor-2 antibody DC101 plus gemcitabine on growth, metastasis and angiogenesis of human pancreatic cancer growing orthotopically in nude mice. *Int J Cancer*, **102**, 101-8.
- Chapet O, Udrescu C, Devonec M, et al (2013). Prostate hypofractionated radiation therapy: injection of hyaluronic acid to better preserve the rectal wall. *Int J Radiat Oncol Biol Phys*, **86**, 72-6.
- Corre I, Niaudet C, Paris F (2010). Plasma membrane signaling induced by ionizing radiation. *Mutat Res*, **704**, 61-7.
- Dimanche-Boitrel MT, Meurette O, Rebillard A, Lacour S (2005). Role of early plasma membrane events in chemotherapy-induced cell death. *Drug Resist Updat*, **8**, 5-14.
- Fuks Z, Kolesnick R (2005). Engaging the vascular component of the tumor response. *Cancer Cell*, **8**, 89-91.
- Garcia-Barros M, Paris F, Cordon-Cardo C, et al (2003). Tumor response to radiotherapy regulated by endothelial cell apoptosis. *Science*, **300**, 1155-9.
- Garcia-Barros M, Thin TH, Maj J, et al (2010). Impact of stromal sensitivity on radiation response of tumors implanted in SCID hosts revisited. *Cancer Res*, **70**, 8179-86.
- Gulbins E, Kolesnick R (2003). Raft ceramide in molecular medicine. *Oncogene*, **22**, 7070-7.
- Haimovitz-Friedman A, Kan CC, Ehleiter D, et al (1994). Ionizing radiation acts on cellular membranes to generate ceramide and initiate apoptosis. *J Exp Med*, **180**, 525-35.
- Hua G, Kolesnick R (2013). Using ASMase knockout mice to model human diseases. *Handb Exp Pharmacol*, **216**, 29-54.
- Kolesnick R, Fuks Z (2003). Radiation and ceramide-induced apoptosis. *Oncogene*, **22**, 5897-906.
- Koukourakis MI, Giatromanolaki A, Tsoutsou P, et al (2011). Bevacizumab, capecitabine, amifostine, and preoperative hypofractionated accelerated radiotherapy (HypoArc) for rectal cancer: a Phase II study. *Int J Radiat Oncol Biol Phys*, **80**, 492-8.
- Lan J, Wan XL, Deng L, et al (2013). Ablative hypofractionated radiotherapy normalizes tumor vasculature in lewis lung carcinoma mice model. *Radiat Res*, **179**, 458-64.
- Li YQ, Chen P, Haimovitz-Friedman A, et al (2003). Endothelial apoptosis initiates acute blood-brain barrier disruption after ionizing radiation. *Cancer Res*, **63**, 5950-6.

- Li ZJ, Zhu H, Ma BY, et al (2012). Inhibitory effect of Bifidobacterium infantis-mediated sKDR prokaryotic expression system on angiogenesis and growth of Lewis lung cancer in mice. *BMC Cancer*, **12**, 155.
- Longo CA, Tyler D, Mallampalli RK (1997). Sphingomyelin metabolism is developmentally regulated in rat lung. *Am J Respir Cell Mol Biol*, **16**, 605-12.
- Moeller BJ, Dreher MR, Rabbani ZN, et al (2005). Pleiotropic effects of HIF-1 blockade on tumor radiosensitivity. *Cancer Cell*, **8**, 99-110.
- Nava VE, Cuvillier O, Edsall LC, et al (2000). Sphingosine enhances apoptosis of radiation-resistant prostate cancer cells. *Cancer Res*, **60**, 4468-74.
- Osti MF, Agolli L, Valeriani M, et al (2013). Image guided hypofractionated 3-dimensional radiation therapy in patients with inoperable advanced stage non-small cell lung cancer. *Int J Radiat Oncol Biol Phys*, **85**, 157-63.
- Paris F, Fuks Z, Kang A, et al (2001). Endothelial apoptosis as the primary lesion initiating intestinal radiation damage in mice. *Science*, **293**, 293-7.
- Park HJ, Griffin RJ, Hui S, et al (2012). Radiation-induced vascular damage in tumors: implications of vascular damage in ablative hypofractionated radiotherapy (SBRT and SRS). *Radiat Res*, **177**, 311-27.
- Pena LA, Fuks Z, Kolesnick RN (2000). Radiation-induced apoptosis of endothelial cells in the murine central nervous system: protection by fibroblast growth factor and sphingomyelinase deficiency. *Cancer Res*, **60**, 321-7.
- Pollard JM, Gatti RA (2009). Clinical radiation sensitivity with DNA repair disorders: an overview. *Int J Radiat Oncol Biol Phys*, **74**, 1323-31.
- Rotolo JA, Maj JG, Feldman R, et al (2008). Bax and Bak do not exhibit functional redundancy in mediating radiation-induced endothelial apoptosis in the intestinal mucosa. *Int J Radiat Oncol Biol Phys*, **70**, 804-15.
- Rotolo JA, Zhang J, Donepudi M, et al (2005). Caspase-dependent and -independent activation of acid sphingomyelinase signaling. *J Biol Chem*, **280**, 26425-34.
- Samet D, Barenholz Y (1999). Characterization of acidic and neutral sphingomyelinase activities in crude extracts of HL-60 cells. *Chem Phys Lipids*, **102**, 65-77.
- Santana P, Pena LA, Haimovitz-Friedman A, et al (1996). Acid sphingomyelinase-deficient human lymphoblasts and mice are defective in radiation-induced apoptosis. *Cell*, **86**, 189-99.
- Saponaro C, Malfettone A, Ranieri G, et al (2013). VEGF, HIF-1alpha expression and MVD as an angiogenic network in familial breast cancer. *PLoS One*, **8**, 53070.
- Stancevic B, Kolesnick R (2010). Ceramide-rich platforms in transmembrane signaling. *FEBS Lett*, **584**, 1728-40.
- Truman JP, Al Gadban MM, Smith KJ, Hammad SM (2011). Acid sphingomyelinase in macrophage biology. *Cell Mol Life Sci*, **68**, 3293-305.
- Truman JP, Garcia-Barros M, Kaag M, et al (2010). Endothelial membrane remodeling is obligate for anti-angiogenic radiosensitization during tumor radiosurgery. *PLoS One*, **5**, 9d04-4d120568a897.
- Utermohlen O, Karow U, Lohler J, Kronke M (2003). Severe impairment in early host defense against *Listeria monocytogenes* in mice deficient in acid sphingomyelinase. *J Immunol*, **170**, 2621-8.
- Xu J, Yan X, Gao R, et al (2010). Effect of irradiation on microvascular endothelial cells of parotid glands in the miniature pig. *Int J Radiat Oncol Biol Phys*, **78**, 897-903.
- Zeidan YH, Hannun YA (2010). The acid sphingomyelinase/ceramide pathway: biomedical significance and mechanisms of regulation. *Curr Mol Med*, **10**, 454-66.
- Zeidan YH, Wu BX, Jenkins RW, et al (2008). A novel role for protein kinase Cdelta-mediated phosphorylation of acid sphingomyelinase in UV light-induced mitochondrial injury. *Faseb J*, **22**, 183-93.
- Zeng H, Yuan Z, Zhu H, et al (2012). Expression of hPNAS-4 radiosensitizes lewis lung cancer. *Int J Radiat Oncol Biol Phys*, **24**, 24.
- Zhang Y, Mattjus P, Schmid PC, et al (2001). Involvement of the acid sphingomyelinase pathway in uva-induced apoptosis. *J Biol Chem*, **276**, 11775-82.
- Zhu H, Li Z, Mao S, et al (2011). Antitumor effect of sFlt-1 gene therapy system mediated by Bifidobacterium Infantis on Lewis lung cancer in mice. *Cancer Gene Ther*, **18**, 884-96.